Twisted split-ring-resonator photonic metamaterial with huge optical activity

M. Decker,[1,*] R. Zhao,[2,3] C. M. Soukoulis,[3,4] S. Linden,[1] and M. Wegener[1]

[1]*Institut für Angewandte Physik and DFG-Center for Functional Nanostructures (CFN), Karlsruhe Institute of Technology (KIT), D-76128 Karlsruhe, Germany, and Institut für Nanotechnologie, Karlsruhe Institute of Technology (KIT), D-76021 Karlsruhe, Germany*

[2]*Applied Optics Beijing Area Major Laboratory, Department of Physics, Beijing Normal University, Beijing 100875, China*

[3]*Ames Laboratory and Department of Physics and Astronomy, Iowa State University, Ames, Iowa 50011, USA*

[4]*IESL-FORTH and Department of Materials Science and Technology, University of Crete, 71110, Heraklion, Greece*

**Corresponding author: manuel.decker@physik.uni-karlsruhe.de*

Received January 21, 2010; revised March 24, 2010; accepted March 31, 2010; posted April 14, 2010 (Doc. ID 123117); published May 6, 2010

Coupled split-ring-resonator metamaterials have previously been shown to exhibit large coupling effects, which are a prerequisite for obtaining large effective optical activity. By a suitable lateral arrangement of these building blocks, we completely eliminate linear birefringence and obtain pure optical activity and connected circular optical dichroism. Experiments around a 100 THz frequency and corresponding modeling are in good agreement. Rotation angles of about 30° for 205 nm sample thickness are derived. © 2010 Optical Society of America

OCIS codes: 160.1585, 160.3918, 220.4241.

Optical activity in effective media refers to a difference $\Delta n = n_{\mathrm{RCP}} - n_{\mathrm{LCP}}$ in the real parts of the refractive indices for left- and right-handed circularly polarized incident light. The Kramers–Kronig relations connect these differences to the imaginary parts of the refractive indices, i.e., to circular dichroism. Optical activity requires a magnetic-dipole response mediated by the electric field of the electromagnetic light wave [1–3]. In natural substances like solutions of chiral molecules, these effects are quite small, i.e., $|\Delta n| \ll 1$. Strong effective magnetic dipoles can arise from the coupling of Mie-like electric-dipole resonances. Coupled gold crosses have recently been discussed in this context [4,5]. Yet stronger coupling effects have been reported for twisted split-ring resonators (SRRs) [6]. However, the latter structures exhibit not only strong optical activity but also strong linear birefringence. A clean separation is desirable for both understanding the physics and for applications such as poor-man's optical isolators [7].

In this Letter, we discuss a lateral arrangement of twisted SRRs that, by symmetry, exhibits vanishing linear optical birefringence. This structure has been mentioned theoretically previously [8] and is discussed in another paper [9] at much larger wavelengths. In contrast to [9], we characterize our chiral structures with the natural optical polarizations, namely, left- and right-handed circular polarization of light corresponding to the eigenpolarizations of the chiral structure. This allows us to unambiguously identify the eigenmodes from the experiment. The circular dichroism measured by us at around 3 μm wavelength translates to values of $|\Delta n| \approx 2$, which outperform our previous best results on twisted crosses [4] by about a factor of six. The twisted SRR pair in [6] exhibits an obvious asymmetry between the x and the y direction. To avoid the resulting linear birefringence, we design a square unit cell that is formed by four of these pairs, wherein the pairs are rotated by 0°, 90°, 180°, and 270° with respect to the stacking axis [see Fig. 1(a)]. The resulting overall crystal structure has fourfold rotational symmetry, no center of inversion, and no mirror planes. Hence, it is truly chiral. We emphasize that the detailed arrangement of the SRR does matter. For example, [10] aims at eliminating circular dichroism and gets linear birefringence. The structure recently published by us [11,12] also exhibits linear eigenpolarizations of +45° and −45°. These facts highlight the importance of the relative arrangement of the SRR pairs for the optical response.

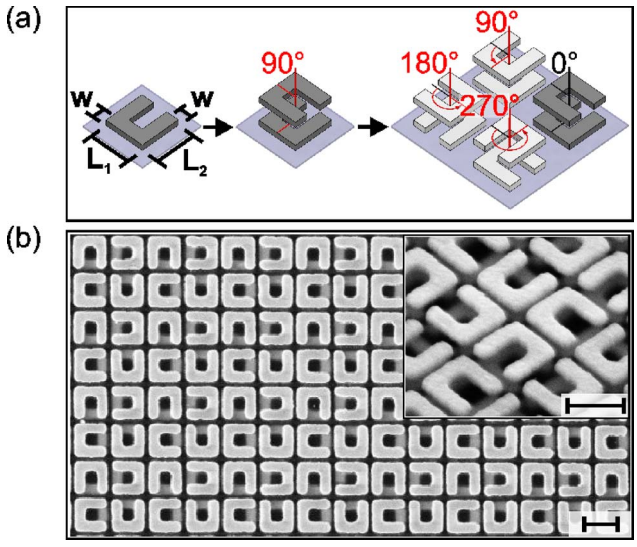

Fig. 1. (Color online) (a) Illustration of our metamaterial's chiral unit cell composed of gold SRRs. The lateral dimensions of the SRRs are indicated on the left-hand side. (b) Electron micrographs of a typical fabricated structure. The normal-incidence image illustrates the high alignment accuracy of the two stacked layers. Inset, oblique view onto the sample. The scale bars are 400 nm.

Fabrication of the two-layer chiral medium shown in Fig. 1 requires advanced nanofabrication, i.e., two successive electron-beam-lithography steps and an intermediate planarization process via a spin-on dielectric [13]. Starting with the first functional layer written by electron-beam lithography, we planarize the sample via a 500-nm-thick spacer layer of commercially available spin-on dielectric (IC1-200, Futurrex, Inc.) and a subsequent thinning via reactive-ion etching (SF_6, Plasmalab80Plus, Oxford Instruments). Next, we process the second functional layer of split-ring resonators via another electron-beam-lithography step carefully aligned relative to the first layer via alignment markers. As a result, we achieve an alignment mismatch of the first and the second layer of below 10 nm over the entire sample footprint of 100 μm $\times$ 100 μm. Electron micrographs of a fabricated structure are shown in Fig. 1(b). The two functional layers are separated by a 85-nm-thick spacer layer. All samples are fabricated on a glass substrate covered with a 5 nm thin film of indium tin oxide (ITO). Obviously, the sample quality is very high. In particular, no misalignment between the two split-ring resonators in each pair is detectable. The in-plane lattice constant of the set of four SRR pairs of $a=885$ nm is significantly smaller than the resonance wavelengths of about 3 μm.

For optical characterization, we use a commercial Fourier-transform microscope spectrometer (Bruker Tensor 27 with Bruker Hyperion 1000) combined with a linear CaF_2 High Extinction Ratio holographic polarizer and a super-achromatic MgF_2-based quarter-wave plate (Bernhard Halle Nachfl., 2.5–7.0 μm) that can be rotated from the outside of the microscope [14]. Furthermore, we have modified the reflective $\times$36 Cassegrain lens (NA=0.5) by introducing a small diaphragm such that the full opening angle of the light incident onto the sample is reduced to about 5°. The sample is tilted such that we achieve actual normal incidence of light onto the sample [14]. Normalization of the transmittance spectra is with respect to the transmittance of the glass substrate, the ITO, and the spacer layer.

The measured transmittance spectra (see Fig. 2) for left-handed circularly polarized (LCP) and right-handed circularly polarized (RCP) light are quite different. Indeed, the observed effects are much stronger compared with our planar chiral metamaterial structure [15] and our twisted-cross metamaterial structure [4]. Precisely, the circular dichroism, i.e., the difference between RCP and LCP transmittance, reaches values of about 33% for the present two-layer twisted SRR metamaterial.

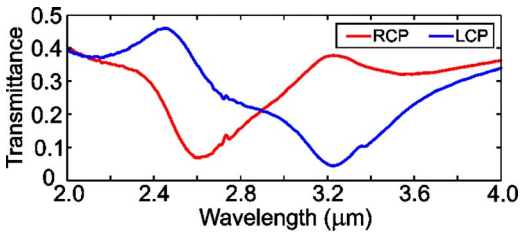

Fig. 2. (Color online) Measured normal-incidence intensity transmittance spectra for LCP and RCP light incident onto the sample shown in Fig. 1(b).

Unfortunately, our experimental setup does not allow for analyzing the emerging polarization of light. To investigate this aspect and to understand the nature of the observed resonances, we perform additional numerical modeling. We use a finite-element frequency-domain approach provided by Comsol MultiPhysics supported by finite-integral time-domain calculations by CST MicroWave Studio. The lateral geometrical parameters of the SRR are $L_1=380$ nm, $L_2=350$ nm, and $w=115$ nm [see Fig. 1(a)]. The gold thickness in each layer is 60 nm, that of the spacer layer 85 nm. The unit cell is arranged in a square lattice with an in-plane lattice constant of $a=885$ nm. The gold optical properties are modeled by a free-electron Drude model with plasma frequency $\omega_{pl}=2\pi\times2133$ THz and collision frequency $\omega_{coll}=2\pi\times33$ THz. The refractive indices of the glass substrate and the spin-on dielectric are 1.45 and 1.41, respectively. The thin ITO film is neglected.

The calculated results in Fig. 3(a) qualitatively agree nicely with our experimental findings in Fig. 2. Furthermore, we find very little intensity conversion (below 10^{-5}) of circular polarization throughout the entire spectral range, i.e., LCP (RCP) incident light emerges as LCP (RCP) transmitted light. This means that LCP and RCP are very nearly the eigenpolarizations of the Jones matrix of our chiral metamaterial structure. Figure 3(b) shows the corresponding calculated rotation angle of linearly polarized incident light, that is, the effects of optical activity. This part of the figure also shows the calculated tangent, e

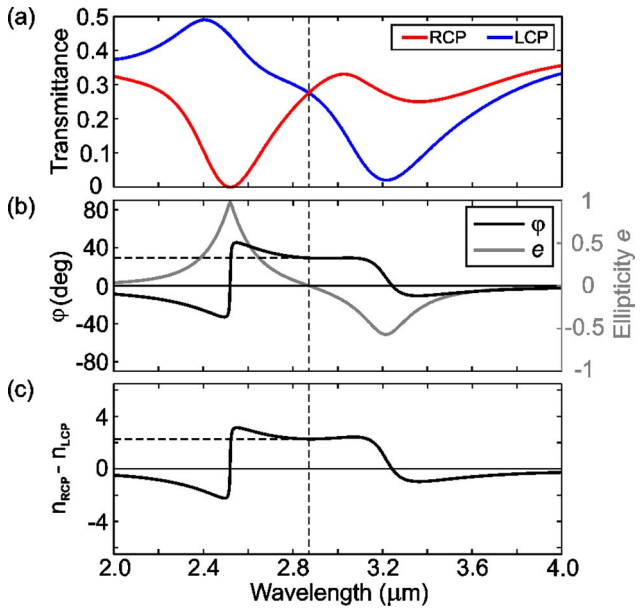

Fig. 3. (Color online) Calculated optical properties. (a) Normal-incidence transmittance spectra that can be directly compared with the experiment shown in Fig. 2. The intensity conversion (not shown) is below 10^{-5} for the entire spectral range. (b) Calculated rotation angle φ and tangent e of the ellipticity angle of the transmitted light for linearly polarized incident light. (c) Difference of refractive indices $\Delta n=n_{RCP}-n_{LCP}$ retrieved from the complex transmittance and reflectance spectra.

$=\tan(\eta)$, of the ellipticity angle η, i.e., the ratio between the semiminor and the semimajor axis of the polarization ellipse. Here $e=0$ corresponds to linear polarization, $e=\pm 1$ to circular polarization. Obviously, the rotation angle φ in Fig. 3(b) exhibits a resonance behavior. In resonance, the ellipticity approaches $e=1$. For pure optical activity we need $e=0$. At this zero crossing in Fig. 3 (dashed line), we find a rotation angle of about 30° for a metamaterial thickness of just 205 nm. Employing the usual parameter retrieval [16] accounting for the glass substrate leads to the difference between RCP and LCP refractive indices $\Delta n = n_{\mathrm{RCP}} - n_{\mathrm{LCP}}$ shown in Fig. 3(c). Values of $|\Delta n| \approx 2$ are found. As expected, the spectral shape of the retrieved index difference Δn closely resembles the rotation angle [Fig. 3(b)] that is directly obtained from the calculated transmission phases.

Finally, we study the nature of the resonances seen in Figs. 2 and 3. The calculated axial component of the local magnetic field is illustrated in Fig. 4. For the low-frequency LCP resonance, the magnetic moments within each SRR pair are obviously parallel. In contrast, for the high-frequency RCP resonance, they are antiparallel. The coupling between the two SRRs in each pair is crucial for the observed optical activity: Without SRR coupling, the frequency splitting between the two modes of the coupled system equals zero. Each individual SRR layer is clearly not chiral; hence no optical activity is observable. Thus, for zero coupling between the two SRR layers, the overall optical response would result from two independent nonchiral layers, leading to an overall nonchiral response. The optimum separation of the two SRR layers results from a trade-off: for too large SRR layer separation, the SRR coupling in each pair vanishes, and so does optical activity. In the other limit, if the two SRR layers lie in the same plane, the structure itself is clearly strictly not chiral [see Fig. 1(a)].

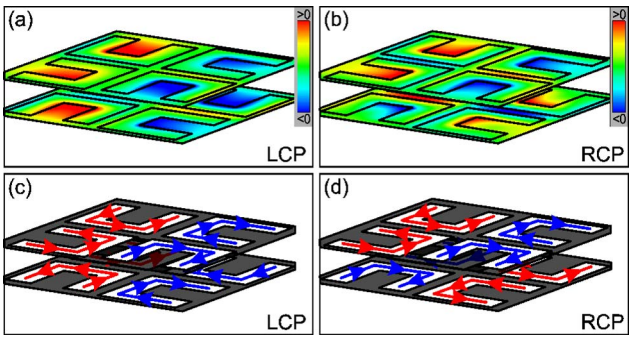

Fig. 4. (Color online) False-color plots of the axial component of the local magnetic field in two planes cutting through the SRR layers for (a) LCP incidence at 3.2 μm wavelength and (b) for RCP incidence at 2.5 μm. Schemes of the corresponding underlying electric currents within the SRR are shown in (c) and (d), respectively.

We have found the SRR separation leading to maximum optical activity by computer simulations. The resulting value of 85 nm for the spacer layer has been used in this Letter.

In conclusion, we have designed, fabricated, and characterized a layer-by-layer chiral metamaterial structure operating at optical frequencies that largely outperforms previous designs regarding the achieved level of optical activity. Around a 3 μm wavelength, we derive rotation angles as large as 30°, corresponding to refractive index differences of about $|\Delta n| \approx 2$.

We acknowledge support by the European Commission via the project PHOME and by the Bundesministerium für Bildung und Forschung via the project METAMAT. The research of S. L. is supported through a Helmholtz-Hochschul-Nachwuchsgruppe (VH-NG-232). The PhD education of M. D. is embedded in the Karlsruhe School of Optics & Photonics (KSOP). Work at Ames Lab was supported by the Department of Energy (Basic Energy Sciences), contract no. DE-AC02-07CH11358.

References

1. E. Plum, J. Zhou, J. Dong, V. A. Fedotov, T. Koschny, C. M. Soukoulis, and N. I. Zheludev, Phys. Rev. B **79**, 035407 (2009).
2. S. Zhang, Y. S. Park, J. Li, X. Lu, W. Zhang, and X. Zhang, Phys. Rev. Lett. **102**, 023901 (2009).
3. M. Wegener and S. Linden, Physics **2**, 3 (2009).
4. M. Decker, M. Ruther, C. E. Kriegler, J. Zhou, C. M. Soukoulis, S. Linden, and M. Wegener, Opt. Lett. **34**, 2501 (2009).
5. J. Zhou, J. Dong, B. Wang, T. Koschny, M. Kafesaki, and C. M. Soukoulis, Phys. Rev. B **79**, 121104 (2009).
6. N. Liu, H. Liu, S. Zhu, and H. Giessen, Nat. Photonics **3**, 157 (2009).
7. M. Thiel, M. Decker, M. Deubel, M. Wegener, S. Linden, and G. von Freymann, Adv. Mater. **19**, 207 (2007).
8. N. Liu and H. Giessen, Opt. Express **16**, 21233 (2008).
9. X. Xiong, W. H. Sun, Y. J. Bao, M. Wang, R. W. Peng, C. Sun, X. Lu, J. Shao, Z. F. Li, and N. B. Ming, Phys. Rev. B **81**, 075119 (2010).
10. X. Xiong, W. H. Sun, Y. J. Bao, R. W. Peng, M. Wang, C. Sun, X. Lu, J. Shao, Z. F. Li, and N. B. Ming, Phys. Rev. B **80**, 201105 (2009).
11. M. Decker, S. Linden, and M. Wegener, Opt. Lett. **34**, 1579 (2009).
12. M. Decker, S. Burger, S. Linden, and M. Wegener, Phys. Rev. B **80**, 193102 (2009).
13. G. Subramania and S. Y. Lin, Appl. Phys. Lett. **85**, 5037 (2004).
14. J. K. Gansel, M. Thiel, M. S. Rill, M. Decker, K. Bade, V. Saile, G. von Freymann, S. Linden, and M. Wegener, Science **325**, 1513 (2009).
15. M. Decker, M. W. Klein, M. Wegener, and S. Linden, Opt. Lett. **32**, 856 (2007).
16. D. H. Kwon, D. H. Werner, A. V. Kildishev, and V. M. Shalaev, Opt. Express **16**, 11822 (2008).